Supporting Information

Low temperature solution processed random silver nanowire as promising replacement for Indium Tin Oxide

Arastoo Teymouri*, Supriya Pillai, Zi Ouyang, Xiaojing Hao, Fangyang Liu, Chang Yan, Martin A. Green

School of Photovoltaic and Renewable Energy (SPREE), University of New South Wales (UNSW), Sydney 2052, Australia

AUTHOR INFORMATION

Corresponding Author

* E-mail: arastoo.teymoori@gmail.com

Figure S1 compares two low temperature methods of heat treatment that were applied in this study. As shown, *in-situ treatment* is able to reduce the sheet resistance at much lower temperatures, than achieved using *post-treatment*.

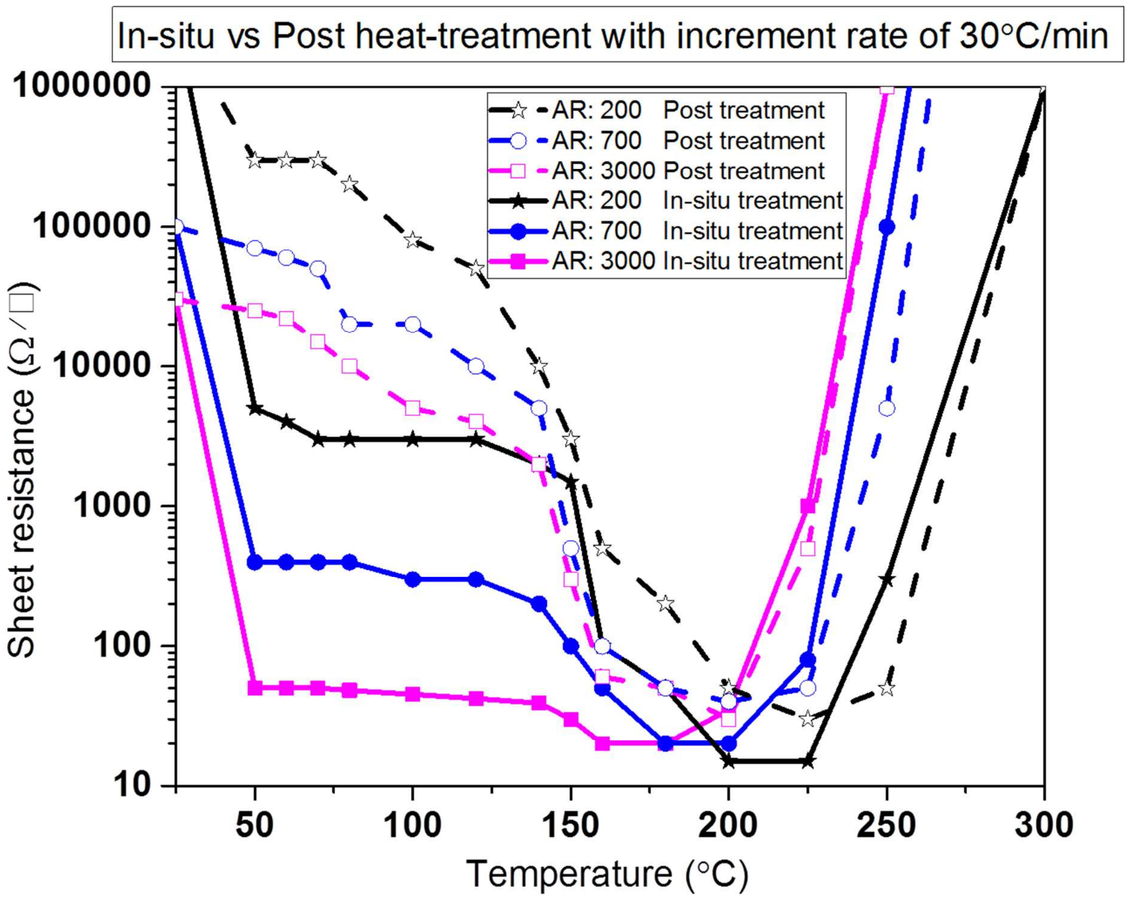

Figure S1. Sheet resistance as a function of temperature for *in-situ heating* and *post-treatment* processes. Dashed lines represent *post-treatment* samples. Solid lines with markers represent *in-situ heating*.

Figure S2 shows the high density of AgNWs network in the area of 20 μm × 20 μm. As is shown, Conductive Atomic Force Microscopy (C-AFM) image is highly compatible with AFM, indicating that the AgNWs network is highly conductive after the low temperature treatment at 60 °C.

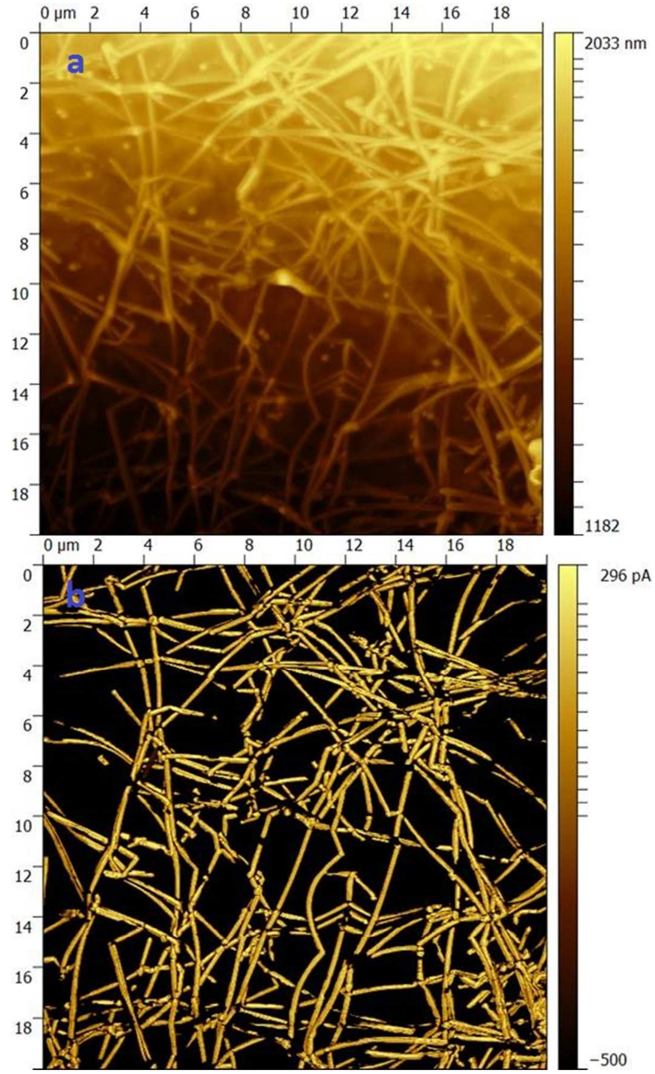

Figure S2. (a) Topographical AFM image of the AgNWs taken from area of 20 μm × 20 μm. (b) C-AFM current map of the same area.

To clearly show how C-AFM could be helpful to prove the conductivity of AgNWs network at microscopic scale, AgNWs was deposited on Polyethylene terephthalate (PET) as substrate with hot plate heating at 60°C. The deposited film was simultaneously pressed in order to partially embed the AgNWs into PET. This process caused some parts of network to break and disconnect from others. Additionally, PET particles could slightly cover the surface of nanowires. The difference between the two images in figure S3 confirms that the pressing AgNWs into PET insulator can disconnect parts of nanowires from the network (blue arrow), which might happen due to either PVP residual in between nanowires at the junctions or broken nanowires (red arrows). On the other hand, this phenomenon can seal the concept that if any point is depicted in the current map, there is undoubtedly a conductive path that can drive electron from that point to the circuit, unless otherwise, that part is disconnected from the network. In other words, every single point depicted in figure S3-b is well connected to the AgNWs network and the charge can traverse to adjacent nanowires, completing the circuit.

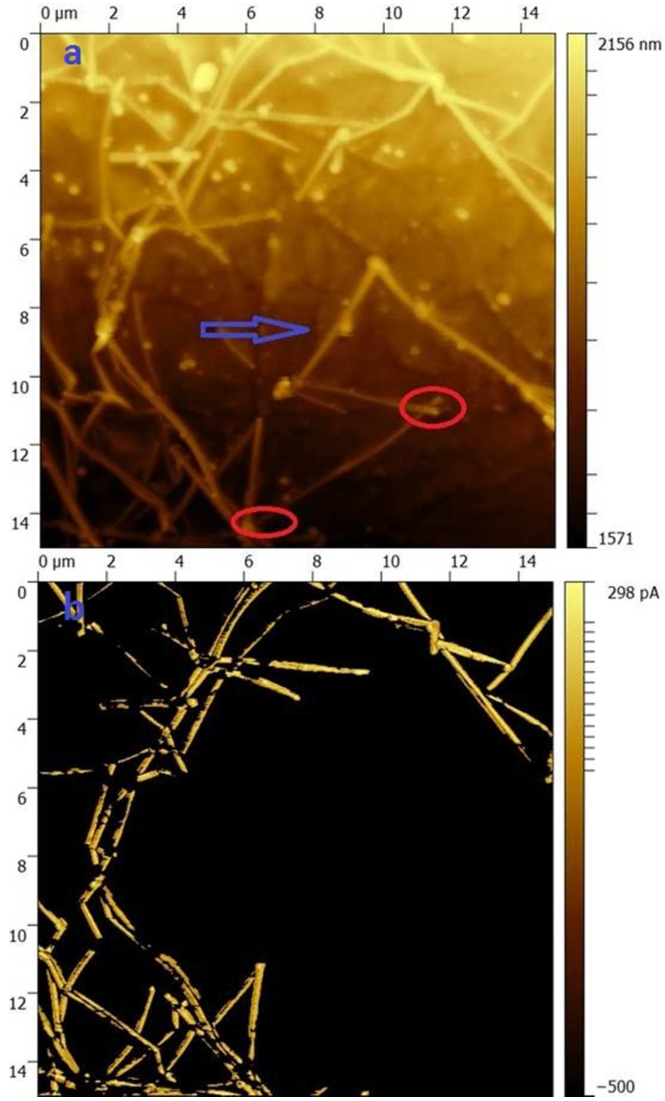

Figure. S3. (a) Topographical AFM image of the AgNWs buried in PET heated at 60 °C, blue arrow shows the isolated part of the AgNWs network, red circles show poor joints of nanowires. (b) C-AFM current map of the same area with no sign of non-conductive part.

Below is the I-V curve measurement of two CZTS cells with the similar process of the production composed of the same components in the absorber layer with different top electrodes. One cell was coated with ITO (thickness: 220nm, sheet resistance: 17.5 Ω/□) and another with AgNWs (200μm long, 70nm wide and sheet resistance: 18 Ω/□) as the window layer. It is clear that owing to the increase of the short circuit current, the efficiency of CZTS with AgNWs as top electrode outperformed the cell with ITO used as top electrode. No significant drop in Voc was observed although further optimisation of the cell properties with AgNW needs to be considered.

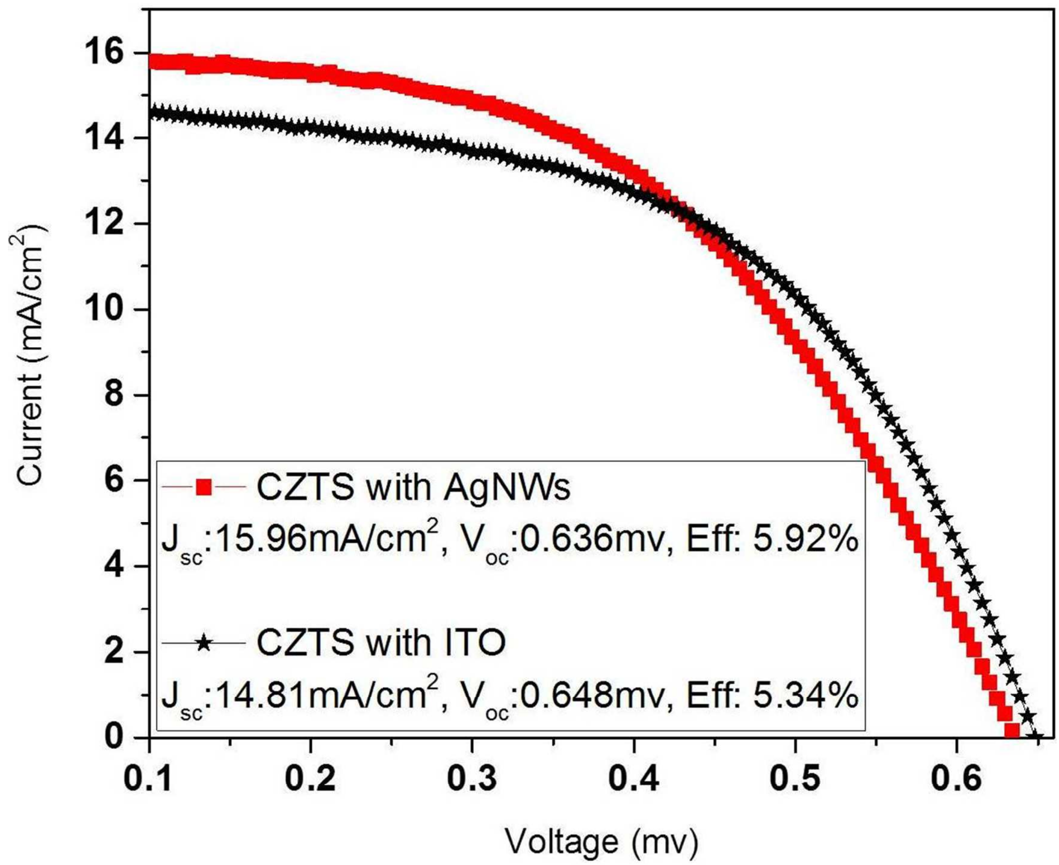

Figure. S4. I-V curve measurement for AgNWs (aspect ratio: 3000) annealed at 60°C (red square markers) and ITO (black star markers) as the top electrode of Kesterite cell.